Author(s): Miettunen, Kati & Asghar, Imran & Ruan, Xiaoli & Halme, Janne & Saukkonen, Tapio & Lund, Peter

Title: Stabilization of metal counter electrodes for dye solar cells

Year: 2011

Version: Post print

Please cite the original version:

Miettunen, Kati & Asghar, Imran & Ruan, Xiaoli & Halme, Janne & Saukkonen, Tapio & Lund, Peter. 2011. Stabilization of metal counter electrodes for dye solar cells. Journal of Electroanalytical Chemistry. Volume 653, Issue 1-2. 93-99. ISSN 1572-6657 (printed). DOI: 10.1016/j.jelechem.2010.12.022.

Stabilization of metal counter electrodes for dye solar cells

Kati Miettunen[*,a], Imran Asghar[a], Xiaoli Ruan[b], Janne Halme[a], Tapio Saukkonen[c], Peter Lund[a]*

[a)] New Energy Technologies Group, Department of Applied Physics, and [c)] Engineering Materials Group, Department of Engineering Design and Production, Aalto University, P.O. BOX 15100, FIN-00076 Aalto, Finland

[b)] College of Materials Science and Engineering, Chongqing University, Chongqing 400045, China

* Corresponding author: kati.miettunen@tkk.fi, +358 50 344 1729

Abstract

The purpose of this study was to identify stable metal based counter electrodes (CE) for dye solar cells (DSC). Previous studies have shown that stainless steel (StS 304) suffers from corrosion when used as a counter electrode. Therefore metals which have inherently higher corrosion resistance, such as stainless steel types 321, 316 and 316L, Inconel 600 and titanium, were investigated here. When using thermal platinization for the preparation of the catalyst layer on CE, only the titanium foil based metal based DSC remained consistently stable in the 1000 h light soaking test. The counter electrodes were also prepared with sputtering ~20 nm thick layer of Pt which provides a highly uniform layer on the CE which acts also as a protective coating on the metal. With sputtered Pt, DSC on all studied metals expect for Inconel remained at 80-95 % of the initial efficiency after light soaking test for 1000 h.

Keywords: dye-sensitized, aging, metal, impedance spectroscopy

1. Introduction

The prominent benefits of dye solar cells (DSC) compared to traditional photovoltaic (PV) technologies are that the DSC can be prepared with cheap materials and using easy manufacturing methods. The most costly component of conventional DSC is the transparent conducting oxide (TCO) layer coated substrate [1]. The costs can be reduced by using metal substrates such as stainless steel (StS) [2,3]. In addition, metals have superior conductivity compared to TCO layers [4-6]. Moreover, for instance StS stands the high temperature treatments used in the production of high quality electrodes. In fact, the highest efficiency of flexible DSC (8.6 %) have been achieved with a metal based DSC [7]. Using flexible substrates such as metals and plastics at both electrodes, roll-to-roll manufacturing could be used for the preparation of DSC important for the commercialization of this emerging PV technology.

The main challenge with many metals such as copper is that they can easily corrode in the iodine containing electrolyte [4,5,8]. StS is practically the cheapest metal that has been stable in electrolyte soaking tests [4,5,8]. Although, it is necessary for a substrate to pass the electrolyte soaking test, it does not guarantee the stability of the substrate in working conditions. In fact in our previous studies, we have detected stability problems when using StS as a photoelectrode [9,10] and as a counter electrode (CE) [11] substrate in DSCs. Interestingly enough, the degradation pattern and apparently also the causes for the degradation are different in those two cases [9-11]. The variation in the degradation is apparently caused by the different potential difference between the electrolyte and the electrode in the case of the two electrodes. Electric potential is known to have a major effect on chemical reactions such as corrosion.

The DSCs with CE based on StS 304 have been stable for a couple of weeks in light soaking tests, but have then suffered from degradation [11]. The degradation of StS CE cells was apparently caused by corrosion as all the typical corrosion marks could be seen at the surface [11]: Iodine typically reacts with

the metal in the case of corrosion which causes then depletion of iodine in the electrolyte [4,5,8,11]. Iodine has a distinct yellow color [12] and because of that, the loss of iodine changes the color of the electrolyte from yellow to transparent [4,5,8,11]. Such a color change occurred in the StS CE cells simultaneously with the performance degradation [11]. Furthermore, scanning electron microscopy (SEM) analysis of the aged StS CE revealed formation of pit holes which are typical for general type of corrosion and apparent corrosion products (metal-iodine compounds) were found in large quantities for instance at the photoelectrode of the StS CE cell [11].

The purpose of this study was to find stable metal based CE for DSC. The metals studied in this work according to their expected corrosion resistance were the following: stainless steel qualities 304, 321, 316 and 316L, Inconel alloy 600, and titanium. Two types of catalyst layers, thermally platinized and sputtered platinum, were tested. The former is a traditional catalyst layer with low coverage and the latter one is a high coverage layer which could potentially be used also as protective layer against corrosion. The stability was tested through a 1000 h light soaking test under 1 sun illumination. Optical characterization, electrochemical chemical impedance spectroscopy (EIS) analysis and SEM imaging of the cells were performed to investigate the photovoltaic performance and the degradation mechanisms in the DSC.

2. Material and methods

2.1. Samples.

The studied metal counter electrode substrates were stainless steels 304 (1.25 mm, Outokumpu Ltd.), 321 (0.05 mm, Goodfellow), 316 (1.25 mm, Outokumpu Ltd.) and 316L (0.05 mm, Goodfellow), Inconel alloy 600 (0.075 mm, Goodfellow), and titanium (0.03 mm). The composition of the studied metals is given in Table 1. Fluorine-doped tin oxide (FTO) coated glass (2.5 mm, Pilkington TEC-15, sheet resistance 15 Ω/sq, Hartford Glass Company, Inc.) was used as a reference counter electrode

substrate and as photoelectrode substrates. The substrates were cleaned with a mild detergent and water followed by three minutes in an ultrasonic bath, first in ethanol and then in acetone. Both thermal platinization using 10 mM $PtCl_4$ in 2-propanol with heating at 385 °C for 15 min [13] and sputtering (Emitech K950X) of Pt (~20 nm) were used for the preparation of the catalyst layers.

FTO-glass based photoelectrodes were prepared by screen printing using a TiO_2 paste (18NR-T, Dyesol). The thickness of the TiO_2 layers was measured with a Dektak 6M stylus profiler (Veeco Instruments) to be about 14 μm. The photoelectrodes were sintered at 450 °C for 30 minutes and then dyed using a solution consisting of 0.32 mM *cis*-bis(isothiocyanato)bis(2,2'-bipyridyl-4,4'-dicarboxylato)-ruthenium(II) bis-tetrabutylammonium (N-719, Dyesol) in ethanol (99.5 wt-%).

The electrodes were attached together with a 25 μm thick Surlyn 1702 ionomer resin film (DuPont) which also served as a spacer. The cells were filled with high stability liquid electrolyte (HSE-EL, Dyesol) and filling holes were encapsuled with a 40 μm thick Surlyn 1601 foil (DuPont) and a thin cover glass. Current collector contacts were made of copper tape which was attached to the electrodes. Conductive silver paint (Electrolube) was applied on the edge of the conductive tape and the substrate to reduce resistance. The electrical contact was reinforced with epoxy glue which needed to dry for 24 h. The structure of the cells was not optimized for high performance.

2.2. Measurements.

Photovoltaic curves were measured using a solar simulator providing 1000 W/m^2 AM1.5G (1 sun) equivalent light intensity at 25 °C and a Keithley 2420 SourceMeter as a potentiostat. The DSC were equipped with black masks with a slightly larger aperture size compared to the active area of the cell which according to literature leads to the most reliable results [14].

The light soaking system composed of halogen lamps (Philips projection lamp, type 13117) providing conditions approximately equivalent to 1 sun at ~40 °C temperature. The open-circuit voltage V_{OC} and short circuit current density i_{SC} were recorded with an Agilent 34980A datalogger in 15 minutes intervals. Complete IV curves were measured once a week with an Autolab PGSTAT302N electrochemical test station.

Electrochemical impedance spectroscopy (EIS) measurements were performed with Zahner Elektrik's IM6 Impedance Measurement unit. The studied frequency range was 100 mHz – 100 kHz and the amplitude was 10 mV. The EIS measurements were taken both under illumination in open-circuit conditions and in the dark in voltage range 0 - -0.7 V. The equivalent circuit analysis of EIS spectra was performed with ZView2 software and commonly used equivalent circuit model [9, 15-18]. The EIS analysis was performed similarly to our previous publications [9,17,18].

A LI-COR LI-1800 spectroradiometer system equipped with an external integrating sphere was employed in the optical measurements. The studied spectral range was 400-1100 nm. As wet and dry samples may have different optical response, the studied counter electrodes were sealed with a microscope glass and 25 μm thick spacer, filled with 3-methoxypropionitrile to mimic the optical characteristics of the CEs in actual DSC.

The aged counter electrodes were examined with a Zeiss Ultra 55 field emission scanning electron microscope (SEM). A 10 kV accelerating voltage was employed in these measurements.

3. Results and Discussion

3.1 Initial performance

The studied DSC were kept over night in dark for preparation reasons. During that time, the color of the electrolyte in the DSC with CE based on StS 304, StS 321 and Inconel with thermal platinization had already bleached completely from deep yellow to completely transparent. The yellow color of the electrolyte is due to tri-iodide in the electrolyte [12] and the color loss relates to the loss of tri-iodide. The loss of electrolyte color is a typical corrosion reaction [4,5,8,11]. The SEM analysis in section 3.5 confirms that the degradation was due to corrosion. The StS 304, StS 321 and Inconel based cells had in fact completely degraded before the first measurements. The rapid degradation of Inconel based CE was particularly unexpected, especially when taking into account that Inconel gave very good stability when used as photoelectrode (PE) substrate in our previous study [10]. The potential difference between the electrolyte and the substrate is different when the substrate is used as a CE or a PE substrate which is known to affect e.g. corrosion and can therefore lead to this kind of situation that stability as a PE substrate does not guarantee stability as a CE substrate. The stability of Inconel is discussed further in section 3.3.

The degradation of StS 304 was similar but significantly faster compared to our previous study with StS 304 based CE when using another electrolyte with low tri-iodide concentration [11]. We suspect that the high tri-iodide concentration in the commercial electrolyte used here could be the reason for the accelerated corrosion in the StS 304 cells since tri-iodide/iodine is typically the corroding agent in the electrolyte [4,5,8,11].

One possible way to prevent corrosion is to use a high coverage protective layer. Hence to improve the stability of the cells, we also employed a sputtered Pt layer (~20 nm thick) which could therefore serve also as a protective layer. The initial results of the sputtered layer were promising since all the cells with the different studied metals with Pt sputtering were functioning in the first measurements (Table 2).

The initial performance measurements were performed on DSC with CE with sputtered Pt layer and with thermal platinization on StS 316, StS 316L, Ti and reference FTO-glass cells. The initial performance is much better, ~20 % higher *FF* and η, with the metal based DSC with sputtered Pt as catalyst layer compared to those with thermal platinization (Table 2). Others have also gained higher *FF* and η, values in case of StS with sputtering than thermal platinization [4]. The reason for low *FF* with thermal platinization on metals is the higher charge transfer resistance (R_{CT}) at counter electrode (Table 2). Our hypothesis is that the surface of the metal oxidizes more during the high temperature treatment required for the thermal platinization. The oxidization of the metals in the high temperature treatment caused a visible change of the substrate color which indicates its significance. The increased oxide layer may then hinder the charge transfer at the CE causing a higher R_{CT}. Contrary to the metal cells, the initial performance of the reference FTO-glass cells is in fact slightly higher with thermal Pt compared to sputtered Pt. The metal and FTO-glass substrate are substantially different: the conducting layer on FTO-glass is an oxide and is generally known to endure around 400 °C temperatures very well, which explains why both high and low temperature techniques work well on FTO-glass.

There was also some small deviation between the different metals which were coated with similar catalyst layer. Some of the variation is caused by slight cell to cell differences e.g. in TiO_2 layer thickness. The substrates have, however, optical difference namely different reflectance which affects back reflection and therefore also i_{SC}. The effect of the optics is discussed in detail in section 3.2.

3.2. Optical analysis

The CE substrate can act also as a back reflector and thus may increase the i_{SC}. The reflectance of the metals depends on the preparation of the metal as the reflectance increases with polishing the surface. The catalyst layer also affects the reflectance as shown in the Figure 1. The reflectance of metal CE with sputtered Pt is 30-50 % in the wavelength range relevant to the N-719 dye (up to ~700 nm). The

thermally platinized metals had lower reflectance than sputtered Pt due to the high temperature treatment which increases the oxidization and changes the color of the metal surface towards brown. This color effect was most evident in case of Ti which also showed very low reflectance with thermal platinization even though Ti with sputtered Pt gave high reflectance similar to the other metals (Figure 1).

We approximate that full back reflection of the light leads to about 15 % higher i_{SC} compared to the case with no back reflection [19]. There were about 10 % differences in the reflectance of the metals with sputtered Pt (Figure 1) which should result in only 1-2 % differences in the i_{SC}. Some correlation can be seen between reflectance and i_{SC}: for instance the highest i_{SC} was reached with StS316L with sputtered Pt which also had highest reflectance (Table 2 and Figure 1b). Some of the small differences in the i_{SC} values between different metals (Table 2) are also due to slight variations in the thickness of the TiO_2 layer.

3.3. Stability of the DSC

As mentioned earlier, StS 304, StS 321 and Inconel with thermal Pt degraded before the initial measurement. The variation in the stability was large in the case of thermally platinized StS 316 and 316L. Some of the StS 316 and 316L samples degraded in a few days, others remained stable for longer times. For instance, the best cell on StS 316 remained quite stable for a few weeks (Figure 2), after which a dramatic drop in i_{SC} led to the complete loss of cell efficiency. Similarly, the best 316L remained stable during the whole studied 6 weeks period (Figure 2). A certain amount of variation in the progress of corrosion is normal which explains why there was some difference in the degradation rates of the 316 and 316L cells. As in the case of cells that had degraded before the initial measurement, all those metal cells which were subject to complete loss of i_{SC} in the long term testing had also a complete loss of electrolyte color. The color change suggests that the degradation was due to corrosion [4,5,8,11].

StS 316 and 316L have increased corrosion resistivity compared to StS 304 and 321 due to an additive, Molybdenum, (Table 1) which explains their better stability in DSC. StS 316L has lesser amount of carbides compared to StS 316 making it more resistant towards corrosion. The only consistently stable metal with thermal Pt catalyst layer was Ti. This is supported by the fact that Ti foil is covered naturally by a thin layer of titanium oxide, making it very stable.

The catalyst layer prepared with thermal platinization does not provide high coverage of the substrate unlike the sputtered Pt layer. With the sputtered Pt catalyst layer which doubles also as a protective coating, the long term stability of the DSC with metal based CE was improved significantly: most of the studied metals maintained 90-95 % of their initial performance during aging under ~1 sun illumination at 40 °C for 6 weeks (~1000 h); only the Inconel based DSC demonstrated complete loss of performance. The StS 304 based DSC degraded more as compared to other DSC with sputtered Pt catalyst. Although the thin (~20 nm) sputtered Pt layers typically have high coverage, they are not pin hole free. Hence, if some metals, such as Inconel, have high tendency towards corrosion as counter electrode substrate, even small gaps in the protective layer may be enough to initiate the notable degradation. The major difference between stainless steels and Inconel is that the former has 70 % of Fe and 8 % of Ni, and the latter has 8 % of Fe and 72 % of Ni (Table 1). When Ni has been tested as such, it has found to corrode in the electrolyte [20]. This implies that the high Ni content of Inconel is the cause of its poor stability. A thicker protective layer might also stabilize Inconel cells. However, as cheaper StS gave better stability compared to Inconel, a more interesting question for further studies from commercial point of view is how thin sputtered Pt layer can be used on StS to get sufficient stability.

Most of the metals with sputtered Pt had very constant i_{SC} (Figure 3), and the slight loss of efficiency (5-10 %) was due to slight decrease in V_{OC} and *FF*. The decrease in V_{OC} is related with increased recombination at the photoelectrode, whereas the decrease in *FF* is associated with increased series

connected resistances such as charge transfer resistances at the CE, diffusion through the electrolyte and charge transfer in the TiO_2 layer. Both the recombination resistance and the series connected resistances are studied in the section 3.5.

3.4 SEM analysis of the aged DSCs

SEM analyses were made of all the metal CEs before and after the cell preparation and the ageing tests. Corrosion pit holes were found on all those metal CE surfaces of aged DSC which experienced complete degradation of i_{SC} and the related loss of electrolyte color. These metals include thermally platinized stainless steels 304, 321, 316, 316L and Inconel, as well as sputtered Inconel. For all other DSC with thermal and sputtered Pt, no changes were detected in the SEM images.

As an example, Figure 4a-b shows the surface of the Pt sputtered Inconel after aging and Figure 4c shows the characteristic features of the Inconel surface before aging. The comparison of the SEM images between the aged (Figure 4a-b) and initial state of surface (Figure 4c), differentiate the features caused by degradation from the characteristic features of Inconel surface. It shows that during the aging, significant change occurred at the surface of Inconel in the form of corrosion pit holes.

Corrosion typically initiates from an imperfection in the metal. Hence, if the metal would have a stable fully covering protective layer, there should not be any corrosion. For example in Figure 4, the corrosion pit holes on the Inconel substrate are therefore likely to be evolved from the parts which have not been covered with the sputtered Pt.

3.5 EIS analysis of the stable DSC

The EIS analysis was performed in accordance to the literature [9,10,15-18]. The equivalent circuit used in the analysis is presented in Figure 5. As explained in detail in the literature [15,17,18], this equivalent circuit (Figure 5) reduces to different simplified circuits depending on the voltage.

The focus of this section is to analyze the performance of only those cells which showed good stability in the light soaking test. The other cells which suffer from huge degradation, resulting in complete loss of performance, did not give stable enough EIS response to be measured. The cause of degradation for those fully degraded cells is quite clear from the SEM analysis and the visible changes in the appearance. Among the cells showing good stability, the EIS response for Pt sputtered StS 316 is presented here as an example (Figure 6). The other DSC including the reference FTO-glass cells which had stayed stable during the light soaking test, showed similar trends in the aging as the example data in Figure 6.

The performance of light-independent series connected components such as R_S and R_{CE}, measured with the same current can be quantitatively compared [10,17,18]. This condition is fulfilled when measurements are made at open circuit condition under illumination. The series resistance R_S, caused mainly by the sheet resistance of the substrates, is given in EIS spectra by the real axis value where the semicircle on the left starts in Figure 6a. It remained unchanged after light soaking test compared to the values measured before the light soaking (Figure 6a-c). The small semicircle on the left in Figure 6a corresponding to the high frequency features in Figure 6b-c, are caused by the charge transfer resistance at the counter electrode / electrolyte interface R_{CE}. Interestingly, R_{CE} had decreased during the light soaking test from 10 Ωcm^2 to 1.5 Ωcm^2, meaning that the catalytic performance of the counter electrode had actually improved (Figure 6a-c). This effect may be caused by the higher temperature in the light soaking (40 °C) which has in the literature caused long term improvements on R_{CE} [21]. The decrease of the R_{CE} should actually result in increase in the fill factor. However, such an effect was not detected. This could be caused e.g. by an increase in the transport resistance R_t of the TiO_2 film. The presence of R_t can

be detected from a slope (45 degree) attached to the semi-circle that relates to R_{CT} [15]. In the data representing the measured after the aging, a small slope related to R_t can be seen in Figure 6a whilst in the before aging data such a clear slope cannot be detected.

The TiO_2 / electrolyte and PE substrate / electrolyte interfaces are parallel connected and here their sum is noted with resistance R_{PE} and capacitance C_{PE}. At large negative voltages R_{CT} dominates whereas at low negative ones R_{SU} dominates the sum of R_{PE}. [15,17,18]. In the data describing open circuit conditions (large negative voltage), the larger semi-circle on the right in Figure 6a and the low frequency response in Figure 6b-c results from the recombination resistance of the TiO_2 to the electrolyte R_{CT}. Figure 6a gives the impression that the R_{CT} has increased during aging. Note however, that a valid comparison of R_{CT} can be made only for data measured at same voltage over the photoelectrode [16-17]. In this case the open-circuit voltage of the cell had slightly decreased during the aging as shown in Figure 3b. As R_{CT} has inverse exponential dependence of voltage, even small decrease in the voltage typically causes a clear increase in R_{CT}.

The R_{PE} data of the initial and aged cells from the dark EIS measurements was analyzed as function of voltage as similar to ref. [10-18]. As an example the DSC with sputtered Pt on StS 316 is shown in Figure 7. The photoelectrodes in all the tested cells were on FTO-glass and their responses were similar to that of other FTO-glass based PE presented in the literature [10,15,17,18]. Comparison of the data of DSC with sputtered StS 316 before and after light soaking test shows that the resistance related to photoelectrode/electrolyte interface had decreased and the related capacitance had increased during aging (Figure 7). The decrease of R_{PE} causes the slight decrease of V_{OC}.

4. Conclusions

In this work, the performance and stability of several different metals were tested as counter electrodes for dye solar cells. Although some of the studied metal based counter electrodes were degraded, stable options were also found. In particular the use of sputtered Pt improved the stability of the most studied metals significantly.

When using thermal platinization, stainless steel (StS) 304, StS 321 and Inconel 600 were seriously degraded even before initial measurements. In the case of StS 316 and StS 316L, there was variation in the lifetime, from a few days to the whole period of 1000 h for light soaking test. All those cells suffered from corrosion. This was indicated by the complete loss of electrolyte color and formation of pit holes shown in the SEM analysis. The only consistently stable metal with thermal Pt was titanium. The high cost of Ti substrates motivated the study of lower cost metals with a protective coating.

When using sputtered Pt (~20 nm thick) which results in high coverage and can hence serve also as a protective coating, the stability of the metal cells improved significantly: the efficiency of the metal based cells remained typically around 80-95 % of the initial value after the 1000 h light soaking test at 40 °C temperature, which was similar to the stability of the reference FTO-glass based cells. Only Inconel 600 showed poor stability with sputtered Pt layer which was likely connected to the high contents of Ni in Inconel. However, application of a sputtered Pt layer on stainless steels 316 and 316L was shown to be a much cheap option compared to using Ti foils to get stable flexible counter electrodes.

Acknowledgement. This study was funded by the Academy of Finland and the National Nature Science Foundation of China (Grant no. 50711130638).

References

[1] J. M. Kroon, N. J. Bakker, H. J. P. Smit, P. Liska, K. R. Thampi, P. Wang, S. M. Zakeeruddin, M. Grätzel, A. Hinsch, S. Hore, U. Würfel, R. Sastrawan, J. R. Durrant, E. Palomares, H. Pettersson, T. Gruszecki, J. Walter, K. Skupien, G.E. Tulloch, Prog. Photo. Volt.: Res. Appl. 15 (2007) 1-18.

[2] K. Zweibel, Sol. Energy Mater. Sol. Cells 59 (1999) 1-18.

[3] A. Payne, R. Duke, R. H. Williams, Energy Policy 29 (2001) 787-800.

[4] T. Ma, X. Fang, M. Akiyama, K. Inoue, H. Noma, E. Abe, J. Electroanal. Chem. 574 (2004) 77-83.

[5] X. Fang, T. Ma, M. Akiyama, G. Guan, S. Tsunematsu, E. Abe, Thin Solid Films 472 (2005) 242-245.

[6] K. Onoda, S. Ngamsinlapasathian, T. Fujieda, S. Yoshikawa, Sol. Energy Mater. Sol. Cells 91 (2007) 1176–1181.

[7] H. Park, Y. Jun, H.-G. Yun, S.-Y. Lee, M. G. Kang, J. Electrochem. Soc. 155 (2008) F145-F149.

[8] M. Toivola, F. Ahlskog, P. Lund, Sol. Energy Mater. Sol. Cells 90 (2006) 2881-2893.

[9] K. Miettunen, J. Halme, P. Lund, J. Phys. Chem. C 113 (2009) 10297-10302.

[10] K. Miettunen, X. Ruan, T. Saukkonen, J. Halme, M. Toivola, H. Guangsheng, P. Lund, J. Electrochem. Soc. 157 (2010) B814-B819.

[11] K. Miettunen, J. Halme, T. Saukkonen, T. Peltola, M. Toivola, P. Lund, Proceedings of the 24th European Photovoltaic Solar Energy Conference (2009) 647-649.

[12] A. Kay, M. Grätzel, Sol. Energy Mat. Sol. Cells 44 (1996) 99-117.

[13] N. Papageorgiou, W.F. Maier, M. Grätzel, J. Electrochem. Soc. 144 (1997) 876-884.

[14] S. Ito, K. Nazeeruddin, P. Liska, P. Comte, R. Charvet, P. Péchy, M. Jirousek, A. Kay, S. Zakeeruddin, M. Grätzel, Prog. Photovolt: Res. Appl. 14 (2006) 581-601.

[15] F. Fabregat-Santiago, J. Bisquert, G. Garcia-Belmonte, G. Boschloo, A. Hagfeldt, Sol. Energy Mater. Sol. Cells 87 (2005) 117-131.

[16] J. Bisquert, G. Garcia-Belmonte, F. Fabregat-Santiago, N. S. Ferriols, P. Bogdanoff, E.C. Pereira, J. Phys Chem. B 104 (2000) 2287-2298.

[17] K. Miettunen, J. Halme, M. Toivola, P. Lund, J. Phys. Chem. C 112 (2008) 4011-4017.

[18] K. Miettunen, J. Halme, P. Vahermaa, T. Saukkonen, M. Toivola, P. Lund, J. Electrochem. Soc. 156 (2009) B876-B883.

[19] K. Miettunen, M. Sc. Thesis, Helsinki University of Technology, Finland, 2006.

[20] G. E. Tulloch, J. Photoch. Photobio. A 164 (2004) 209-219.

[21] M. Toivola, J. Halme, L. Peltokorpi, P. Lund, Int. J. Photoenergy (2009) 786429.

Table 1. The chemical composition (%) of different stainless steels and Inconel according to the data supplied by the manufacturer.

	Fe	Cr	Ni	Mo	Co	Others
StS 304	balance	18.1	8.1			C
StS 321	balance	18	9			Ti, C
StS 316	balance	17.2	10.1	2.1		C
StS 316L	balance	18	10	3		C
Inconel 600	8	16	72		balance	Mn, Si, C, S

Table 2. Typical initial performance characteristics of the cells with different counter electrode substrates with thermal platinization and with sputtered Pt catalyst layers.

substrate	i_{SC} (mA/cm^2)	V_{OC} (mV)	*FF* (%)	η (%)	R_{CT} (Ωcm^2)
Thermal Pt					
FTO-glass	11.8	659	63	4.92	9
StS 316	11.4	652	50	3.71	38
StS 316L	10.7	634	53	3.60	43
Ti	11.5	643	46	3.41	71
Sputtered Pt					
FTO-glass	11.2	665	62	4.62	9
StS 304	11.4	637	66	4.75	11
StS 321	10.9	636	66	4.57	11
StS 316	11.9	660	64	5.11	10
StS 316L	12.1	655	63	4.93	15
Inconel	11.5	633	64	4.65	11
Ti	11.3	631	67	4.79	9

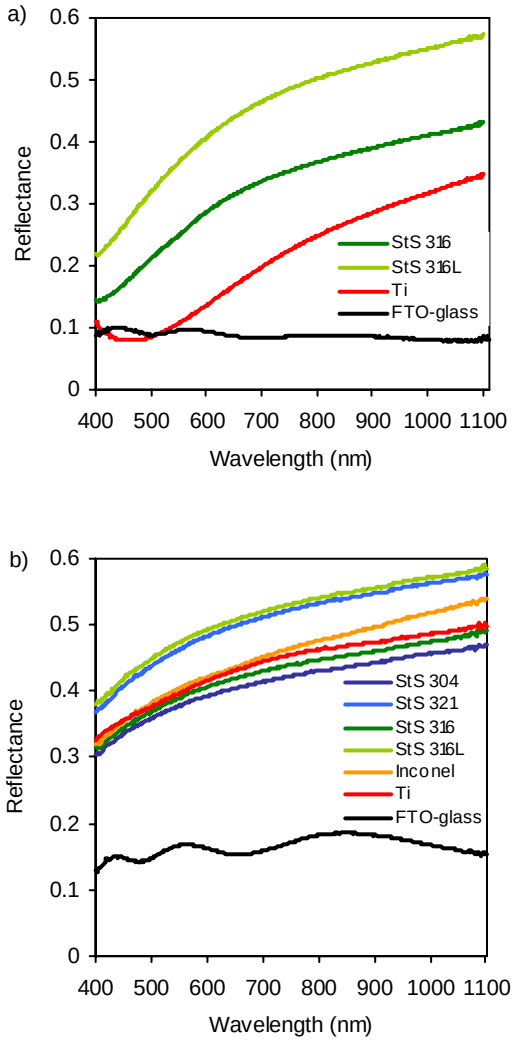

Figure 1. Reflectance of different counter electrodes with a) thermal platinization and b) with sputtered Pt.

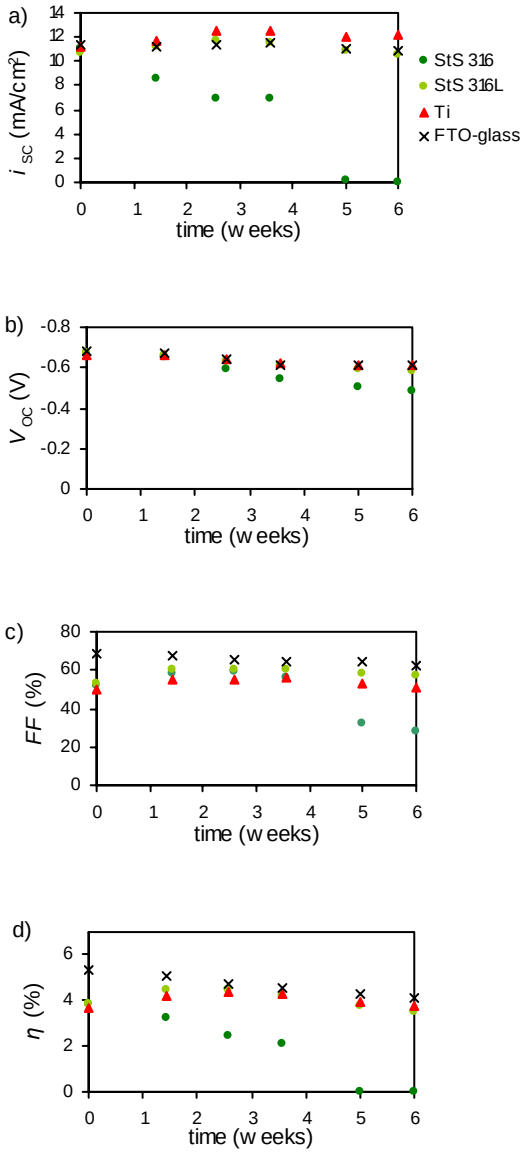

Figure 2. a) short-circuit current density i_{SC}, b) open circuit voltage V_{OC}, c) fill factor *FF* and d) efficiency η as a function of time in the best cells with different metals as counter electrode substrate and thermal Pt catalyst layer. Cells with 304, 321 and Inconel with thermal platinization had degraded before the initial measurement.

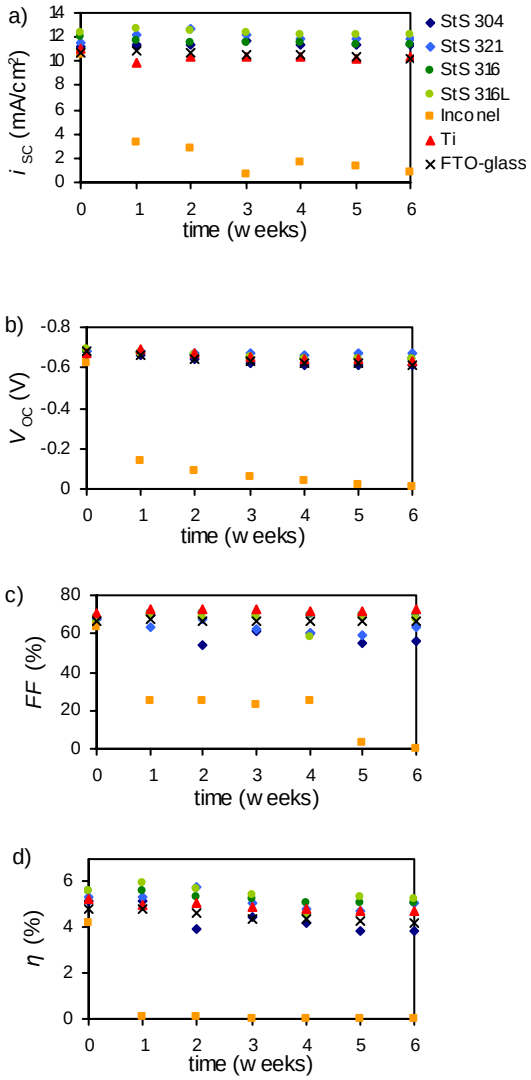

Figure 3. Typical a) short-circuit current density i_{SC}, b) open circuit voltage V_{OC}, c) fill factor *FF* and d) efficiency η as a function of time in the cells with different metals as counter electrode substrate and sputtered Pt catalyst layer. In b) all curves except for Inconel are overlapping.

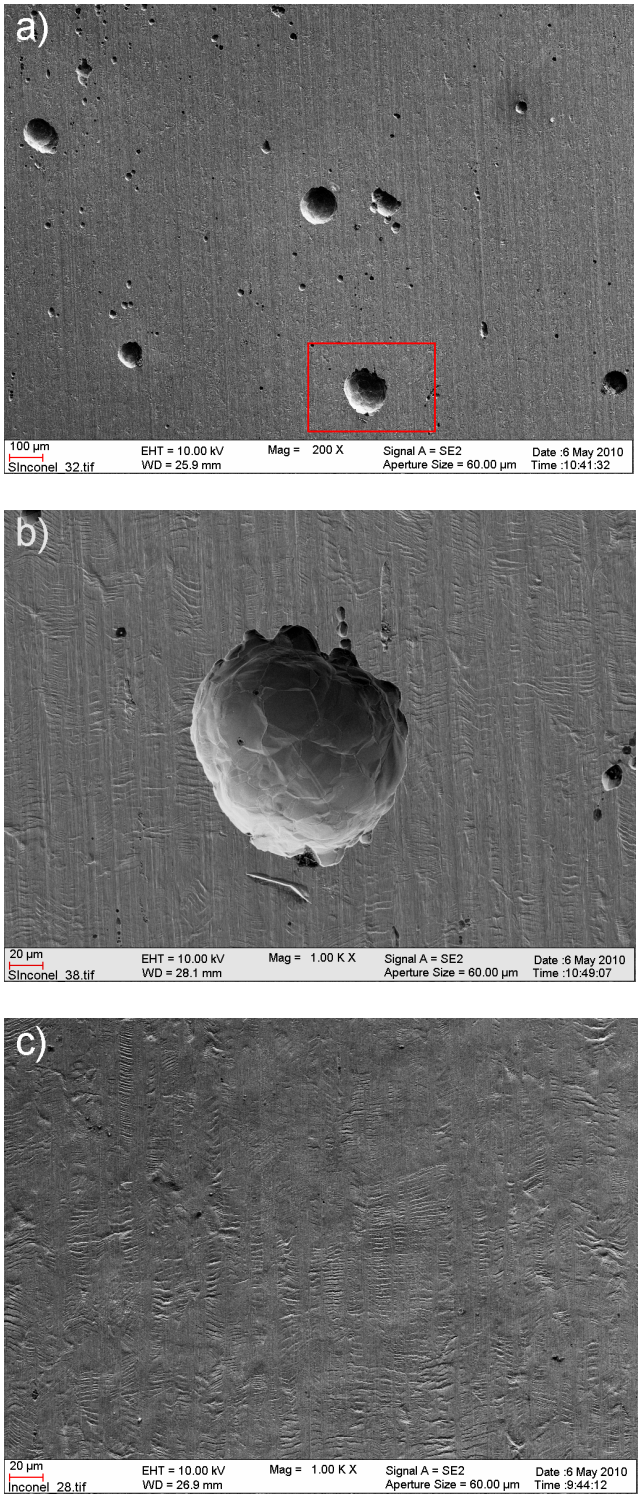

Figure 4. a) A SEM image of a sputtered Inconel substrate from a degraded cell. b) A magnification of a corrosion pit hole from the area which is marked with the rectangle in figure a. c) Reference SEM image of a Inconel substrate in initial condition.

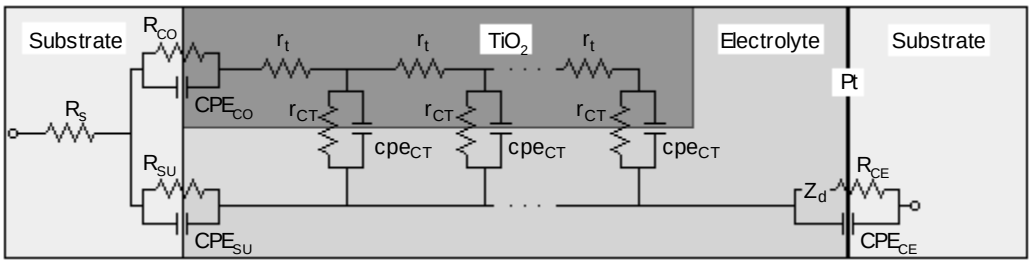

Figure 5. Equivalent circuit model of a DSC [9,10,15-18]: R_S is the ohmic series resistance. R_t (= $r_t d$) is the electron transport resistance and d is the thickness of the layer. Z_d is the mass transfer impedance at the counter electrode caused by ionic diffusion in the electrolyte There are also several constant phase element (CPE) / resistor (R) pairs which are related to different interfaces denoted in the subscript: SU the PE substrate / electrolyte, CO the PE substrate / the porous TiO_2, CT the TiO_2 / electrolyte interface, and CE the counter electrode/electrolyte.

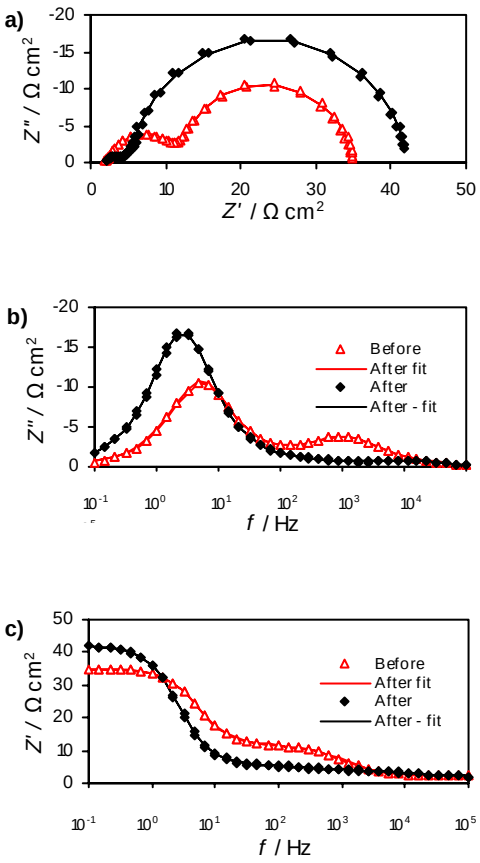

Figure 6. EIS response of a DSC with sputtered StS 316 as a counter electrode before and after the light soaking test measured under illumination at open circuit conditions. The data is shown as a) a Nyquist plot b) imaginary impedance *Z''* vs. frequency *f* and c) real impedance *Z'* vs. *f*.

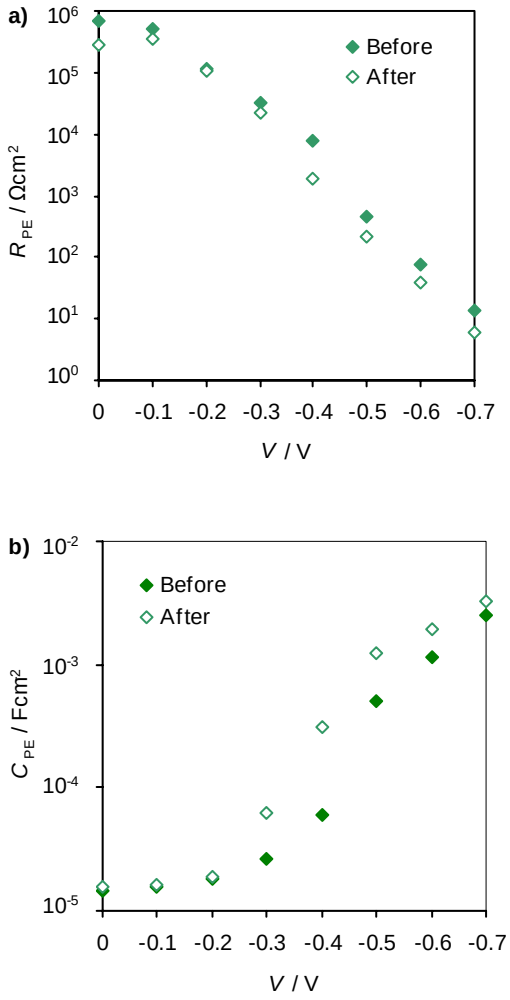

Figure 7. a) Resistance R_{PE} and b) capacitance C_{PE} caused by the parallel connected TiO_2 / electrolyte and PE substrate / electrolyte interfaces in a DSC with Pt sputtered StS 316 as a counter electrode before and after the light soaking test measured by EIS in the dark.